Laboratory Studies of Binary Salt CVD in Combustion Gas Environments

A flash-evaporation technique is used to obtain vapor deposition characteristics for the binary alkali sulfates $K_2SO_4 + Na_2SO_4$ at 1 atm above 1,100 K. This technique gives results of immediate engineering interest, such as dewpoint temperatures, condensate composition and rates of vapor deposition as well as useful data on the system's thermodynamic characteristics. It is concluded that alkali sulfate deposition and vaporization in combustion environments are inevitably influenced by chemical reactions such as hydroxide formation. It is also concluded that solution nonideality is important even for homologous alkali-salt mixtures.

Predictions are made using convective-diffusion mass transfer theory, accounting for chemical reactions by means of effective volatilities, and assuming regular, nonideal condensate solutions. The predicted dewpoints, condensate compositions and deposition rates are quantitatively consistent with experimental observations. This approach, validated here, can be extended to more extreme conditions of engineering interest, including turbulent, high-temperature/pressure systems.

Baishen Liang, D. E. Rosner
Department of Chemical Engineering
High-Temperature Chemical Reaction Engineering Laboratory
Yale University
New Haven, CT 06520

Introduction

For diverse reasons, increasing attention has been paid to chemical vapor deposition (CVD) in high-temperature flow systems in the past two decades (Powell et al., 1966; Stearns et al., 1983). For example, it was realized that the useful life of a high-performance combustion turbine engine in a marine environment, and hence the system economics, is often dictated by the deposition rate of corrosive trace inorganic salts (e.g., Na_2SO_4) whose vapor precursors are inevitably present in the combustion products. As another technological driver, the CVD of thin solid films has become important to the semiconductor industry for the preparation of microelectronic chips. These and other technologies have stimulated a number of papers dealing with both experimental and theoretical aspects of CVD (Robinson et al., 1985; Rosner et al., 1979; Rosner and Nagarajan, 1985; Seshadri and Rosner, 1984); however, many of these papers have been confined to the deposition of a single-species condensate [e.g., pure $Na_2SO_4(l)$, pure $Si(s)$, etc.]. A few authors have performed laboratory experiments on the deposition of multicomponent condensates (Stevens and Tidy, 1983), investigating the effects of other impurities in fuel, such as calcium or potassium, on the deposition rate of the main impurity, say sodium. For example, it was found that additional impurities could reduce the threshold concentration of Na-containing species for the existence of its stable condensate. Unfortunately, such findings have apparently not attracted enough attention nor stimulated much further work, perhaps partly due to the complexity of the thermodynamic system investigated and the high cost of the test techniques.

Multicomponent condensate cases deserve much further study because of their practical importance. For instance, most fuel oils contain sodium and vanadium compounds. Many impurities containing Na, Ca, Al, Si, and other elements are also present in coal; typically, coal contains about 10 wt.% mineral matter. Moreover, inorganic materials are often introduced as combustion additives. Examples are dolomite as a sulfur getter and potassium salts for electrical conductivity control in magnetohydrodynamic (MHD) combustion systems. Note that multicomponent chemical vapor transport processes take place in each of these cases (Hastie, 1975, 1981).

A convenient experimental technique for studying multicomponent deposition rate phenomena, the flash-evaporation tech-

Correspondence concerning this paper should be addressed to D. E. Rosner.
Baishen Liang is presently at the Department of Chemical Engineering, University of California, Berkeley, CA 94720.

nique, is being developed at this laboratory. [Our use of the word "flash" (see also Rosner and Liang, 1986) should not be interpreted to imply "instantaneous"; rather we abruptly initiate a rapid evaporation process at a constant ribbon temperature in the absence of alkali vapor in the mainstream.] The preliminary results for binary alkali sulfate condensate systems reported here indicate that this experimental technique meets most of the research requirements for studying multicomponent systems of current interest. The simple experimental equipment and procedures we have developed thus far are described in the next section. The various deposition rate effects of introducing additives, and our experimental inference of condensate composition, are then presented, followed by a discussion of these findings and their theoretical implications. The final section offers important conclusions concerning binary alkali sulfate solution nonideality and vapor phase decomposition/chemical reactions. Results under more complex conditions (including binary vapor condensation within the boundary layer) and a corresponding theoretical analysis are presented in separate papers (Liang, 1987; Liang et al., 1987; Castillo and Rosner, 1986a–d).

Flash-Evaporation Technique

As introduced in our previous paper emphasizing unary system CVD (Rosner and Liang, 1986), in the flash-evaporation experimental procedure we first allow an alkali-containing salt to be acquired for about 10 min on a platinum ribbon target immersed in seeded combustion products. We then flash-evaporate this initial inventory of condensate into the ribbon wake by raising the ribbon temperature well above the prevailing dewpoint temperature, using Joule (electrical) heating. The alkali compounds partially dissociate in the wake of the ribbon to form alkali atoms, the excited part of which emit radiation at their characteristic wavelengths. Thus, simultaneous, noninterfering measurement of these alkali elements is possible in the wake of the deposition target during the flash evaporation portion of the deposition/flash sequential experiment.

Apparatus

The experimental arrangement is shown in Figure 1. Essentially, it consists of a combustion gas supply system, nebulizer-aerosol producer, flat flame burner, Pt ribbon target with electrical power supply, and optical signal detector.

The present experiments are performed using premixed gaseous $C_3H_8 + O_2 + N_2$ supplied to a seeded flat flame burner operating at atmospheric pressure. The flat flame burner, fabricated from a 3.5 cm ID stainless steel tube, is fed at its base. Variable-area flowmeters are used to measure gas flow rates. To stabilize the flame of premixed gases and obtain a uniform laminar flow of combustion products above the burner, a stainless steel honeycomb disk is placed on its top. Flame temperature and stability are controlled by the proper combination of each gas flow. Mainstream temperatures reported in this paper are estimated from Pt/Rh thermocouple measurements corrected for radiation losses from the thermocouple junction surface.

The platinum ribbon, which serves as our deposition target, is 5 mm wide and 0.127 mm thick. Its surface is parallel to the vertical laminar flow of combustion products and the ribbon is held horizontally above the burner by two copper rods connected to a d.c. power supply so that its temperature can be controlled by varying the electrical power supplied. The brightness temperature at the central part of the ribbon is measured with an optical pyrometer (Pyrometer Instrument Co., Bergenfield, NJ).

An ultrasonic nebulizer is used to generate a highly dispersed aqueous solution aerosol that is transported into the burner by a carrier stream of nitrogen. The nebulizer itself consists of a par-

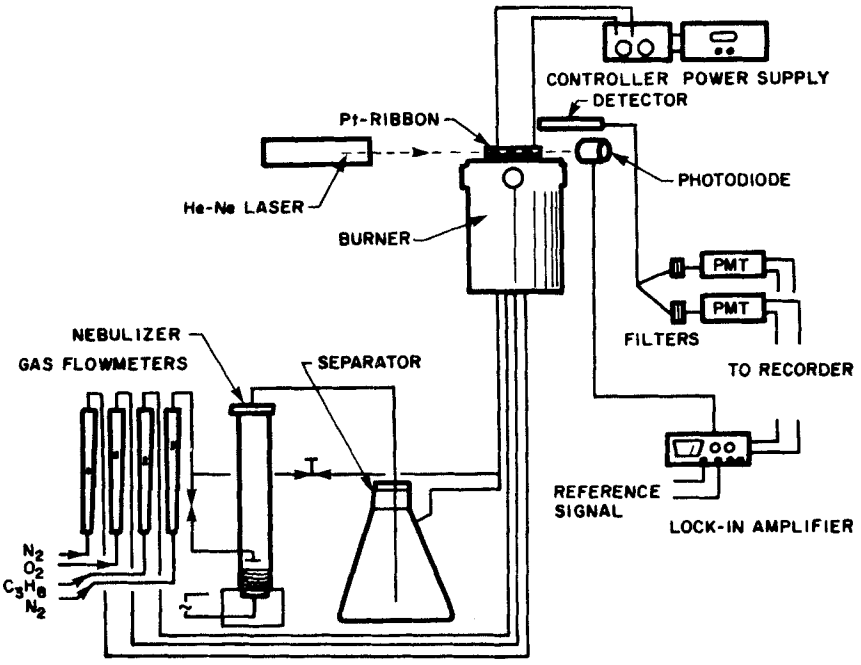

Figure 1. Experimental set-up to study binary salt mixture deposition rate processes.
Laser shown used to probe BL (Rosner and Liang, 1987)

tially liquid-filled vertical glass cylinder, 30 cm long by 3 cm dia., at the base of which a 2 cm dia. piezoelectric transducer is mounted, driven by a variable power RF generator supplying power at the resonant frequency (1.35 MHz) of the crystal. It is estimated that the mean droplet diameter produced by the nebulizer is about 3 μm.

A stream of nitrogen is used to elutriate the alkali-salt containing aerosol out of the nebulizer, first into a series of two plenum chambers to sediment any agglomerated droplets and damp any flow unsteadiness, and from there to the point of mixing with precombustion gases supplied to the burner. In the flame, we experimentally verified that each aerosol droplet is vaporized before the combustion gas stream encounters the ribbon target. This was done by first setting the detector probe at the intended height of the target ribbon, and measuring the emission intensity of one salt, say potassium sulfate, at the maximum solution concentration to be used in our experiments. When a second salt, sodium sulfate for instance, is added to the solution contained in the nebulizer (keeping the concentration of potassium sulfate constant), the same aerosol droplet size is expected because the addition of trace salts does not appreciably change the physical properties of the nebulizer liquid. However, upon water vaporization a mixed alkali sulfate aerosol is thereby formed, which should take longer to evaporate its potassium content. Experimentally, we found that the potassium atom line emission intensity was constant despite increasing sodium sulfate concentration, implying that the alkali vaporization of each aerosol droplet is essentially complete well before the height under observation and that chosen for the target location. (When the sodium sulfate concentration exceeded a certain value, a reduction of potassium emission intensity was observed. Beyond this point droplet vaporization is probably incomplete, so these conditions were not investigated.)

For our deposition rate measurements, an optical detector probe is placed in the wake of the ribbon target, receiving a signal from the emitting alkali atoms in the flame gases. The position and collimation of this probe must be carefully selected to prevent the emission background of the Pt target from entering the detector. The optical train used consists of a lens, optical fiber (3.2 mm dia., Edmund Scientific Co.), beam splitter, and narrow band pass interference filters (Ditric Optics, Inc.). By splitting the beam into more than one part we can measure different species at the same time. In the present experiments the binary potassium sulfate-sodium sulfate system is studied. Accordingly, two filters, 765 nm for potassium and 589 nm for sodium, are simultaneously used here. After passing through the filters, the two light beams enter two photomultipliers (EMI 9635 and 9558), respectively, supplied with high voltage power (EMI model 3000R). Finally, the photomultiplier outputs are fed to picoammeters (EMI 1012) and recorded by a four-pen strip chart recorder (Linseis LS4). Figures 2a and 2b give flash curve examples for the single K_2SO_4 condensate and the K_2SO_4/Na_2SO_4 mixture, respectively.

Experimental procedure

After adjusting the combustion gases to predetermined flow rate values [typically $\dot{V}(N_2)$ = 1,520 (to nebulizer) cm^3/min; $\dot{V}(N_2)$ = 1,840 cm^3/min; $\dot{V}(O_2)$ = 3,170 cm^3/min; $\dot{V}(C_3H_8)$ = 170 cm^3/min (at 293 K, 1 atm)], they are ignited. Initially, by adjusting the voltage imposed across the ribbon, the ribbon target is maintained at a temperature of about 1,470 K, well above

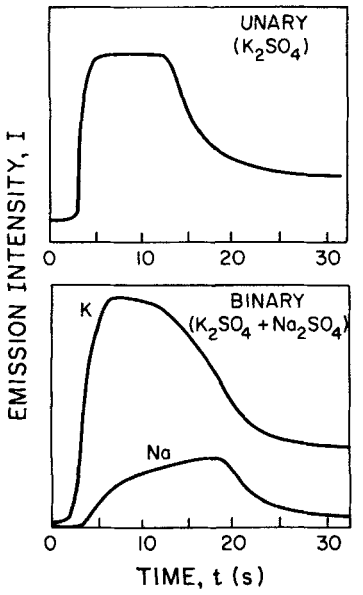

Figure 2. Examples of recorded flash curves.
Single, K_2SO_4 (top)
Mixture of K_2SO_4 and Na_2SO_4 (bottom)

the dewpoint temperature of the alkali sulfates involved, to flash and clean the target surface.

After stabilizing the flame and the output of the signal generator for driving the nebulizer, the ultrasonic nebulizer is turned on and the aerosol of the aqueous solution with its carrier gas, N_2, is directed into the flame. When a stable picoammeter output is observed, the ribbon temperature is abruptly reduced to a desired value, 1,100–1,250 K (in < 0.1 s), by dropping the imposed voltage. If the new steady temperature is below the species dewpoint, then a portion of the condensible material present in the flame diffuses to, and is deposited on, the target surface. In our present experiments, this deposition stage is of fixed duration, about 10 min, after which the nebulizer is turned off and the carrier gas is switched through the bypass into the burner. Therefore, the flame seed level is dropped to zero.

When the optical signal decays to its baseline value, the temperature of the target is abruptly raised to the flash temperature, for example, 1,465 K, so that all of the predeposited condensate inventory is vaporized. During this flash the alkali atom emission intensity vs. time curves are monitored, Figure 2.

The resulting data consist of a recording of the atomic emission intensity vs. time at a series of target temperatures for each seed level, at different concentrations of aqueous solutions of the sulfate salt mixture fed into the burner. Calculation of the area between the recorded emission curve and the baseline gives a result proportional to the total amount accumulated in the deposition stage for the corresponding species.

For each primary salt seed level in the combustion gases, the calculated deposition rate decreases with increasing target temperature, and increases with increasing the level of second-salt impurity. We plot both the experimentally observed deposition rate relationships and extrapolate the resulting curves to obtain values of the dewpoint, defined as the first target temperature (approach from below) at which a condensate becomes unstable with respect to vaporization. In this way we have determined the relation between the dewpoint temperature and the concentration ratio of K_2SO_4 and Na_2SO_4 in the aqueous solution feed.

For a more detailed account of this flash-evaporation technique, with emphasis on unary salt experiments, the reader can refer to our previous paper (Rosner and Liang, 1986).

Results

Binary salt deposition rate measurements

Figure 3 shows the inferred deposition rate of potassium sulfate with the addition of sodium sulfate to the same mainstream (together with the predictions of vapor diffusion boundary layer theory to be discussed later). In these experiments, the concentration of the primary salt, K_2SO_4, is kept constant by holding the concentration of potassium sulfate aqueous solution in the nebulizer at 0.0125 M. In Figure 3, the ordinate is the K_2SO_4 deposition rate normalized relative to the deposition rate of pure K_2SO_4 at T_w = 1,200 K, and the abscissa is the ratio of $[Na_2SO_4/K_2SO_4]$ in the feed. The zero deposition rate intercepts shown plotted were obtained by a somewhat different procedure in which we searched for the reported dewpoints at constant values of the salt ratio (see also Figure 5). We see that the K_2SO_4 deposition rate increases with small additions of Na_2SO_4 to the mainstream (i.e., increasing the ratio of $[Na_2SO_4/K_2SO_4]$ at each target temperature level). This trend is readily understood in terms of the following argument.

It is expected that a binary solution is formed on the "cold" surface upon adding the second condensible species, Na_2SO_4, provided that the target surface temperature is below the dewpoint of the mixture in the prevailing combustion gases. The composition of the condensate and the deposition rate are expected to depend on the surface temperature and the partial vapor pressure of each condensible species in the mainstream. The presence of the second salt lowers the partial vapor pressure of the first salt in the vapor phase above (in local equilibrium with) the condensed solution phase. Therefore, the driving force (associated with the primary salt vapor concentration difference across the boundary layer) increases. The resulting deposition rate trend is in qualitative agreement with the experimental results collected in Figure 3. The same would occur for the reciprocal experiment (K_2SO_4 addition to a Na_2SO_4-seeded flame), but the effect would be less pronounced because of the lower volatility of sodium sulfate. A more quantitative comparison will be discussed later.

It might appear that nothing unusual would happen if the

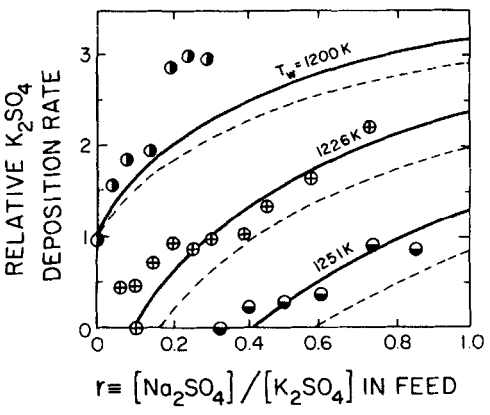

Figure 3. Deposition rate of K_2SO_4 in K_2SO_4/Na_2SO_4 binary system.
0.0125 M K_2SO_4 in nebulizer solution; flash temp., 1,465 K

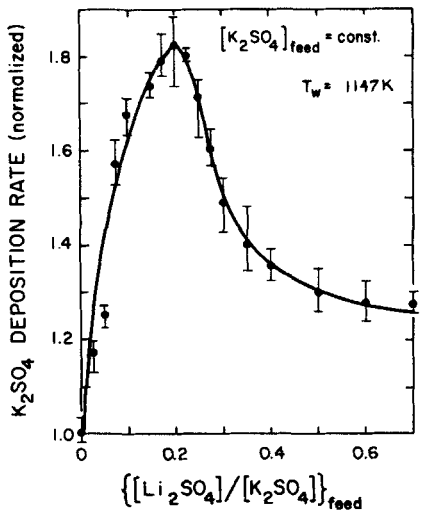

Figure 4. K_2SO_4 deposition rate trends in K_2SO_4/Li_2SO_4 binary system.

content of the second species were increased further. In fact, the second salt need not be Na_2SO_4 but another alkali salt, for example Li_2SO_4, for which we also ran exploratory experiments. Figure 4 shows the deposition rate of potassium sulfate in the binary K_2SO_4/Li_2SO_4 system, with the concentration of K_2SO_4 in the nebulizer solution again being held constant at 0.0125 M. When the $[Li_2SO_4/K_2SO_4]$ ratio in the feed is relatively low, the deposition rate of potassium sulfate increases with increasing ratio addition of lithium sulfate, behaving the same as shown in Figure 3. But, remarkably, the deposition rate decreases rather abruptly with a further increase of the content of lithium sulfate when the salt ratio is larger than a threshold value (near 0.18 in this example). This interesting behavior, clearly contrary to the above-mentioned predictions of vapor diffusion boundary layer theory, will require a more comprehensive physical model. Since supersaturations with respect to the solution condensate may be achieved in the vapor phase near the cold target surface, with increasing second salt seed level such supersaturations could become high enough to reach a critical value for mist formation. Such nucleation would reduce the net potassium sulfate deposition rate due to the smaller capture efficiency for the newly formed particles. Based on this physical picture, confirmed by recent experiments in which we detected the light scattered by the mist particles (Liang et al., 1987), a theoretical model has also been developed to quantitatively predict deposition processes in binary systems beyond the threshold for vapor phase condensation (Castillo and Rosner, 1987d). Deposition under such conditions is the subject of a separate paper (Liang et al., 1987).

Influence of an added mainstream salt on the dewpoint

The presence of a second alkali salt in the mainstream not only changes the deposition rate but also significantly affects the dewpoint temperature. Put another way, the presence of a second alkali salt changes conditions for the existence of a stable condensate phase. By making a plot of deposition rate vs. target temperature at different concentration ratios we obtain the values of dewpoint temperatures by extrapolating the deposition rate curves to zero.

The dewpoint data shown in Figure 5 must be compatible

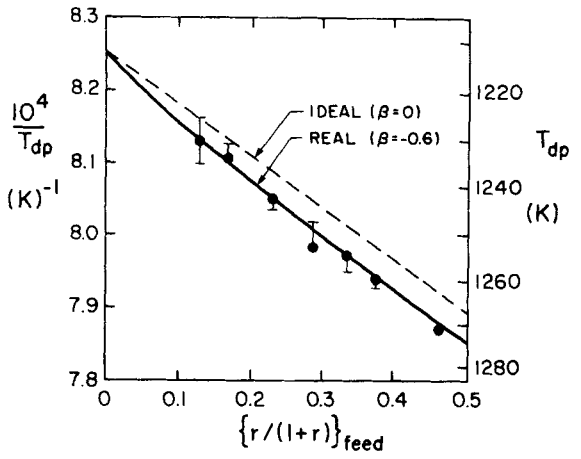

Figure 5. K_2SO_4/Na_2SO_4 mixture dewpoint temperature.
0.0125 M K_2SO_4 in nebulizer solution
● Experiment; — prediction, nonideal solution model; --- prediction, ideal solution model

with zero deposition rate intercepts of the data shown in Figure 3; however, in actually carrying out experiments near the reported dewpoints we kept r = const. and varied the ribbon temperature above and below. The reciprocal of the inferred dewpoint temperature is taken as the ordinate, the alkali salt ratio in the nebulizer solution, $f \equiv [Na_2SO_4]/([Na_2SO_4] + [K_2SO_4])$ is the abscissa. Our experimental results show that the dewpoint temperature of the mixture increases dramatically with increasing Na_2SO_4 addition. For example, when $f = 0.375$ condensates appear below $T_{dp} = 1{,}260$ K; when $f = 0.130$, condensates appear below $T_{dp} = 1{,}230$ K. This implies that the presence of a second mainstream salt vapor enlarges the temperature interval for a thermodynamically stable solution deposit.

Condensate composition

Using the method discussed below we can estimate the composition of the binary solution condensate formed on our ribbon specimens. In what follows it is assumed that the variation of the salt content of the feed gas has no effect on the host flame thermodynamics because of the low salt concentration. We measure a series of emission intensity of potassium and sodium, I_K and I_{Na}, in seeded flames of known concentrations under the flash flame conditions. Considering the emission background (from both flame and target surface), we use $I_K - I_{K,0}$ and $I_{Na} - I_{Na,0}$ and make a plot of $(I_{Na} - I_{Na,0})/(I_K - I_{K,0})$ vs $[Na_2SO_4/K_2SO_4]$ in the nebulizer solution, as shown in Figure 6. By assuming no interference between the two emission measurements and negligible self-absorption, a linear relationship exists. In the present case this can be simply expressed:

$$\frac{I_{Na} - I_{Na,0}}{I_K - I_{K,0}} = S\,\frac{[Na_2SO_4]}{[K_2SO_4]}$$

where S is the dimensionless proportionality constant. We adopt the procedure described previously to measure the relative inventories of Na_2SO_4 and K_2SO_4, $\int_0^\infty I_i\,dt$, predeposited on the target. The ratio of those two species in the condensed solution is obtained by using the above calibration curve. For a binary system the composition of the previously deposited solution is then calculable. Figures 7a and 7b present the observed relation

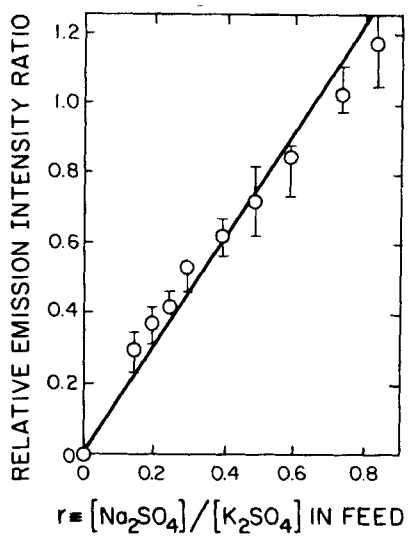

Figure 6. Calibration curve for determination of condensate composition.

between condensate composition and feed composition at each target temperature (and a comparison with the predicted relation, including solution nonideality; see below). Not surprisingly, the content of Na_2SO_4 in the deposit increases with increasing Na_2SO_4 concentration in the feed. On the other hand, the relative Na_2SO_4 content increases with increasing deposition temperature because of its lower volatility relative to K_2SO_4.

Discussion

Analysis of flash curve to infer solution thermodynamics of mixed sulfates

When the target surface temperature is abruptly raised to, and maintained at, the flash temperature (about 1,465 K in our experiments), the predeposited condensate inventory is vaporized. Figure 2a, which is a flash curve for single K_2SO_4 condensate evaporation, shows a typical curve having a flat-top shape, implying that there was an interval of nearly constant evaporation rate. However, when a multicomponent solution mixture is flashed, the curves observed look quite different even though the process proceeds under the same constant ribbon temperature

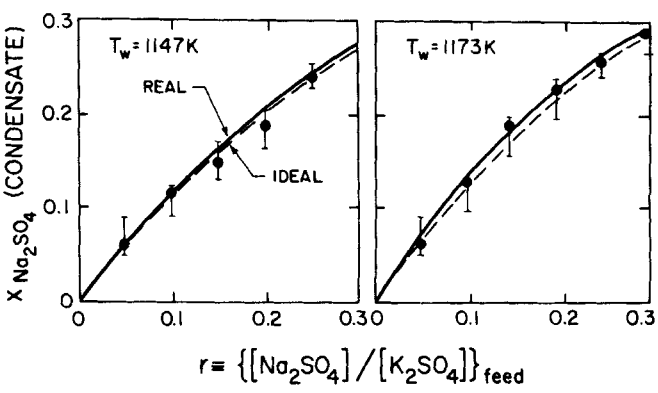

Figure 7. Experimentally inferred and theoretically predicted condensate composition.
— Prediction, nonideal solution model; --- prediction, ideal solution model

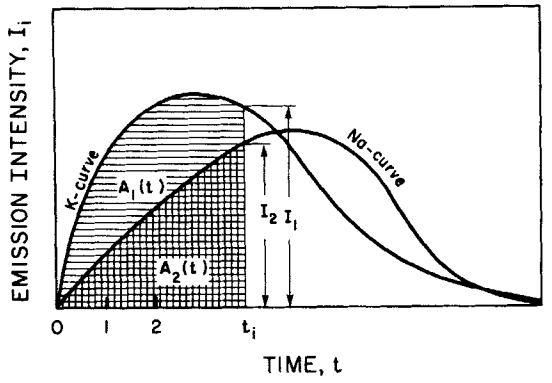

Figure 8. Illustration of emission curve analysis

conditions. Figure 2b gives another flash curve for a K_2SO_4/Na_2SO_4 mixture the sodium sulfate mole fraction of which is about 0.23 just before flashing. The cause for this shape change is the changing composition of condensate (on which the evaporation flux depends) on the target surface during the flash. In addition, inspecting the pair of curves directly, we immediately find that the highest peak of sodium sulfate has a time delay compared with that for potassium sulfate, even when the original composition of sodium sulfate exceeds 50%. This is essentially due to the volatility difference (potassium sulfate is more volatile than sodium sulfate; a quantitative discussion is given later). Thus, the flash curves not only give us global deposition rate results (using total areas), but also offer additional instantaneous information about deposit composition evolution during the flash. Quantitative information about the thermodynamics of such solutions can therefore be obtained by treating the curves in the following way: First, we divide the area, $\int_0^\infty I_i(t)\,dt$, defined by the curve and baseline into strips corresponding to equal time intervals, as shown in Figure 8. As described previously, the total area is proportional to the condensed amount collected during the deposition stage,

$$A_i(\infty) = \int_0^\infty I_i(t)\,dt \propto \int_0^{\tau_T} (-\dot{J}_i'')\,d\tau,$$

where τ_T is the deposition period. Therefore the initial composition of condensed binary solution is

$$x_2(0) = \frac{A_2(\infty)}{SA_1(\infty) + A_2(\infty)}$$

Here, S is a sensitivity coefficient for emission intensity measurement defined by

$$\frac{[K_2SO_4]}{[Na_2SO_4]} = S \cdot \frac{(I_K - I_K^0)}{(I_{Na} - I_{Na}^0)}$$

where I_i^0 is the signal background measured in the case without seeding. In the emission intensity measurement for the species concentration range of interest there is good linearity; that is, S is nearly a constant, Figure 6. After time t in the flash stage, the instantaneous composition of inventory remaining on the target is

$$x_2(t) = \frac{A_2(\infty) - A_2(t)}{S[A_1(\infty) - A_1(t)] + [A_2(\infty) - A_2(t)]} \qquad (1)$$

where $A_i(t)$ is the "running" integral:

$$A_i(t) \equiv \int_0^t I_i(t)\,dt, \quad (i = 1, 2)$$

and we label K_2SO_4 as species 1 and Na_2SO_4 as species 2. Furthermore, to compare experimental results with predictions we define a fraction-evaporated function

$$f_i \equiv \frac{A_i(t)}{A_i(\infty)} \qquad (i = 1, 2) \qquad (2)$$

In order to establish a theoretical relation between f_1 and f_2, we assume that during the flash evaporation process:

1. A mist-free vapor boundary layer exists
2. Local thermodynamic equilibrium is achieved at the condensate-covered target surface where the vapor can be treated as an ideal gas
3. There is a negligible partial pressure of sulfate vapors in the mainstream, that is, $p_{i,\infty} = 0$
4. Quasi-steady state evaporation takes place

Then at each instant the molar flux of each evaporated species can be expressed

$$\begin{aligned} -\dot{J}_i'' &= K_{m,i}[p_{i,w} - p_{i,\infty}] \\ &= K_{m,i}p_{i,w} \\ &= K_{m,i}p_i^0 a_i \end{aligned} \qquad (3)$$

where a_i is the thermodynamic activity of species i. Finally, we assume that:

5. The condensate inventory is a binary, homogeneous (single-phase) molten salt solution and we wish to infer the extent to which such molten salt solutions are thermodynamically nonideal

Other investigators have found that the thermodynamics of these melts are well represented using "regular" nonideal solution theory (Turkdogan, 1980; Blander, 1964; Lumsden, 1966). For binary salt mixtures with a common anion, the activity coefficient γ_i and the molar heat of solution ΔH^{mix} for the mixture obeying the regular solution law are given by

$$\begin{aligned} \gamma_i &= \exp(\beta x_j^2) \\ \Delta H^{mix} &= RT\beta x_i x_j \end{aligned} \qquad (4)$$

where β is the so-called interaction parameter (dimensionless), T is the temperature in K and R is the universal gas constant. $RT\beta$ does not vary much with temperature. Ostvold and Kleppa (1971) measured the enthalpy of mixing of binary solution of Na_2SO_4 and K_2SO_4 by calorimetric techniques and, when T = 1,353 K, $x_{Na_2SO_4} = x_{K_2SO_4} = 0.5$, they reported $\Delta H^{mix} = -0.2625$ kcal/mol. On this basis it may be estimated that the β value is approximately -0.45 in the temperature range of interest here. However, the parameter can be determined independently by fitting our own flash-evaporation data, as shown below.

For the binary system, the convective-diffusion controlled evaporation flux ratio of K_2SO_4 and Na_2SO_4 in the flash stage is accordingly

$$\begin{aligned} \frac{-\dot{J}_1''}{-\dot{J}_2''} &= \left(\frac{D_1}{D_2}\right)^{2/3} \frac{p_1^0\gamma_1 x_1}{p_2^0\gamma_2 x_2}, \\ &= \left(\frac{D_1}{D_2}\right)^{2/3} \alpha_{12} \frac{1 - x_2}{x_2} \exp(2\beta x_2 - \beta) \end{aligned} \qquad (5)$$

where it has been supposed that $K_{m,1}/K_{m,2} \approx (D_1/D_2)^{2/3}$ for the case $Sc > 1$. Here, $\alpha_{12} \equiv p_1^0/p_2^0$ is the volatility ratio of these two sulfates.

As indicated above, the molar flux, $-\dot{J}_i''$, is a function of time, t, during the flash and is directly related to instantaneous emission intensity,

$$\frac{-\dot{J}_1''}{-\dot{J}_2''} = S\frac{I_1}{I_2} \tag{6}$$

Here S is a sensitivity-ratio constant, as defined before. Therefore, Eq. 5 can be rewritten as:

$$\frac{I_1}{I_2} = \frac{1}{S}\left(\frac{D_1}{D_2}\right)^{2/3}\alpha_{12}\frac{1-x_2}{x_2}\exp(2\beta x_2 - \beta) \tag{7}$$

Substituting Eqs. 1 and 2 into Eq. 7, we obtain

$$\frac{I_1}{I_2} = \left(\frac{D_1}{D_2}\right)^{2/3}\alpha_{12}\frac{(1-f_1)A_1(\infty)}{(1-f_2)A_2(\infty)} \cdot \exp\left(\beta\frac{(1-f_2)A_2(\infty) - S(1-f_1)A_1(\infty)}{S(1-f_1)A_1(\infty) + (1-f_2)A_2(\infty)}\right) \tag{8}$$

Now, in principle, we can predict the relationship between f_1 and f_2 provided that α_{12} and β are known because the other parameters, I_i, $A_i(\infty)$, S, etc. are obtained from experimental measurement. Conversely, we can use the experimental f-locus data to estimate the important parameters α_{12} and β. Here, the least-squares method has been used by defining a function

$$E(\alpha_{12},\beta) = \sum_i^N\left(\frac{I_{1,i}}{I_{2,i}} - R_i\right)^2$$

$$R_i = \left(\frac{D_1}{D_2}\right)^{2/3}\alpha_{12}\frac{(1-f_{1,i})A_1(\infty)}{(1-f_{2,i})A_2(\infty)} \exp\left[\beta\frac{(1-f_{2,i})A_2(\infty) - S(1-f_{1,i})A_1(\infty)}{Se(1-f_{1,i})A_1(\infty) + (1-f_{2,i})A_2(\infty)}\right]$$

Taking partial derivatives with respect to α_{12} and β, respectively,

$$\frac{\partial E}{\partial \alpha_{12}} = 0, \quad \frac{\partial E}{\partial \beta} = 0$$

and solving these equations, we found that for $\alpha \approx 1.5, \beta \approx -0.6$, the predicted behavior fit our experimental observation quite well. Figure 9a is inferred by analyzing a flash curve of a condensed inventory having initial Na_2SO_4 mole fraction 0.23 and Figure 9b for initial Na_2SO_4 mole fraction 0.46. Some important implications of these figures (volatility ratio near unity and interaction parameter corresponding to slight nonideality) are discussed below.

Chemical interaction between alkali sulfate vapors and combustion products

From the results of the analysis in the preceding section, we immediately face an apparent paradox: why is our inferred volatility ratio for K_2SO_4 and Na_2SO_4 so close to unity? This conclusion appears to conflict with a series of papers on pure sulfate vapor pressures (Kohl et al., 1979; Fryxell et al., 1973; Cubicciotti and Keneshea, 1972; Janz et al., 1979; Gorokhov, 1975; Hastie, 1981; Cutler, 1983; Lau et al., 1979) published in the last twenty years. Even though there are some significant differences among them and each has a limited accuracy, the average ratio of $p^0_{K_2SO_4}$ and $p^0_{Na_2SO_4}$ in the temperature range 1,100 ~ 1,500 K from these references is about 10 ~ 30, that is, very far from the value 1.5 inferred above from our binary flash experiments. In Figure 10, however, which shows our measured dewpoints in each unary system, the apparent volatility ratio appears to be only about 2.5.

We show below that this apparent disparity can be explained in terms of chemical reactions between the present alkali sulfates and inevitable constituents of the hydrocarbon fuel combustion products.

As several authors have already mentioned, sulfates decompose in chemically reactive environments. (Kohl et al., 1979; Lau et al., 1979). For example, in addition to the physical vaporization process expressed by the reaction

$$M_2SO_{4(c)} = M_2SO_{4(g)} \tag{R1}$$

the following (decomposition) chemical reactions are usually cited as important

$$M_2SO_{4(c)} = 2M_{(g)} + SO_2 + O_2 \tag{R2}$$

$$M_2SO_{4(c)} = M_2O_{(g)} + SO_2 + \frac{1}{2}O_2 \tag{R3}$$

$$M_2SO_{4(c)} = M_2O_{(g)} + SO_3 \tag{R4}$$

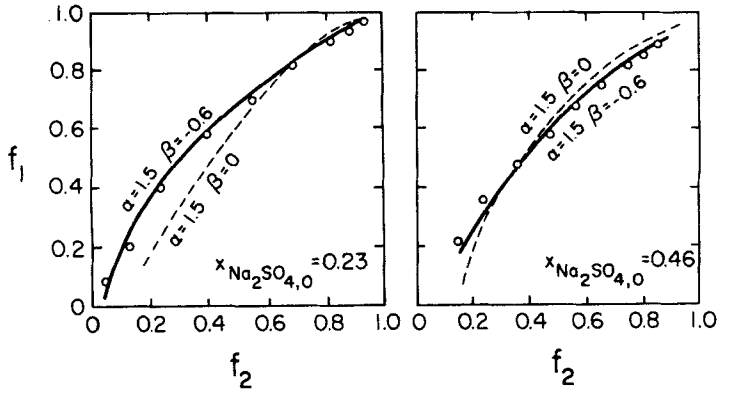

Figure 9. Flash curve analysis for K_2SO_4 + Na_2SO_4 binary condensate mixture.
Deposition temp., 1,150 K; flash temp., 1,465 K

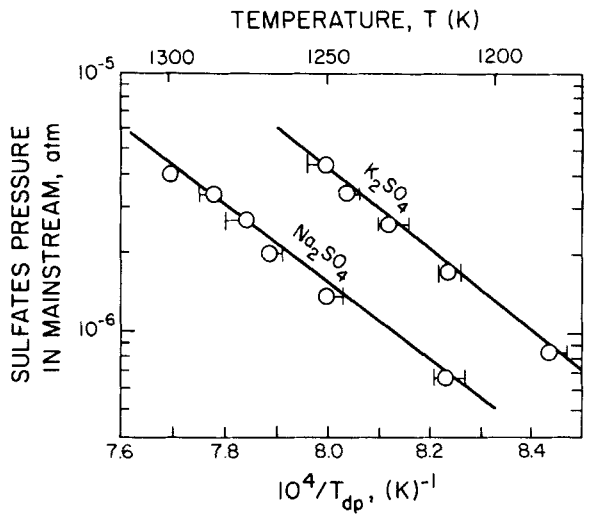

Figure 10. Experimentally inferred dewpoint temperature-seed level relation.
Single species (K_2SO_4 or Na_2SO_4) in combustion product environment

along with the further dissociation reactions

$$SO_3 = SO_2 + \frac{1}{2}O_2 \qquad \text{(R5)}$$

$$M_2O_{(g)} = 2M_{(g)} + \frac{1}{2}O_2 \qquad \text{(R6)}$$

$$M_{2(g)} = 2M_{(g)} \qquad \text{(R7)}$$

(It should be realized that while these reactions are representative of the chemistry, they are by no means a complete set of all elementary reactions taking place.) Here subscript c indicates condensed phase, subscript g gas phase, and M is the alkali element. It is found from mass spectrometric investigations that decomposition reaction R2 is significant in the range of temperature and pressure of interest here.

However, account must also be taken of the fact that in hydrocarbon fuel combustion products water vapor and carbon dioxide will be produced (in our experiments H_2O is also introduced from the aqueous solution alkali feed), and these will also influence the vaporization equilibrium of sulfates. Therefore one must consider reactions such as

$$M_2SO_{4(g)} + CO_2 = M_2CO_{3(g)} + SO_2 + \frac{1}{2}O_2 \qquad \text{(R8)}$$

$$M_2SO_{4(c)} + H_2O = 2MOH_{(g)} + SO_2 + \frac{1}{2}O_2 \qquad \text{(R9)}$$

Using the torsion-effusion method and mass spectrometry, Lau et al. (1979) found that at a temperature near 1,200 K, $p_{K_2SO_4}/p = 0.63$, where p is the total pressure in the system. Their finding can be simply explained as follows. Suppose in a closed system the only decomposition is reaction R2. Assuming the activity for condensed species is unity, and the gases are ideal, then the reaction equilibrium constant can be written $K = p_M^2 p_{SO_2} p_{O_2}$, where $p_{SO_2} = \frac{1}{2}p_M = p_{O_2}$. Thus $K = 4p_{SO_2}^4$.

Table 1. Na_2SO_4 Decomposition

Species i	ΔG^0 1,200 K	ΔG^0 1,300 K	ΔG^0 1,460 K
$Na_2SO_{4(l)}$	−213.612	−199.93	−178.305
$Na_{(g)}$	0	0	0
SO_2	−65.582	−63.84	−61.662
O_2	0	0	0
$\ln K = -(\Delta G^0/RT)$	−62.08	−52.68	−40.21
$p_{SO_2} \times 10^7$	1.29	13.4	305
$p_{Na_2SO_4}\, 10^7$	0.693	5.84	136
$p^c_{Na_2SO_4} \times 10^7$	1.983	19.24	441

Based on JANAF data we calculate the equilibrium vapor pressure for each species as shown in Tables 1 and 2. Then, the total pressure can be defined $p = p_{K_2SO_4} + p_K + p_{SO_2} + p_{O_2}$. At a temperature of 1,200 K, $p \simeq 10.4 \times 10^{-7}$ atm and $p_{K_2SO_4}/p \simeq 0.65$, which is consistent with Lau's measurements.

Under our experimental conditions, however, there is an excess of oxygen. It is estimated that the partial pressure of O_2 in combustion products would be about 0.34 atm. In this case decomposition reaction R2 is strongly suppressed. For instance, at T = 1,460 K the partial pressure of SO_2 is $p_{SO_2} = ([K/4p_{O_2})]^{1/3}$, 0.136×10^{-5} atm for Na_2SO_4 and 0.858×10^{-6} atm for K_2SO_4. This implies that the contribution of decomposition reaction R2 is negligible under our present conditions.

On the other hand, the high partial pressure of H_2O in combustion gases enhances reaction R9, leading to gaseous MOH. Using a free-energy minimization technique (Gordon and McBride, 1976), we calculated all significant equilibrium products and the resulting composition for our experimental system. As an example, we tabulate the equilibrium composition for one case in Table 4, the input for which is close to our experimental conditions, see Table 3.

As can be seen from Table 4, accurate prediction of condensible species transport processes in a high-temperature, chemically reactive environment are inevitably complicated by the fact that a spectrum of products may form in the vapor phase because of chemical reactions with the combustion products and partial dissociation of the condensate constituents. Thus, species in the gas phase generally include not only the undissociated vapor of the salts that eventually deposit (e.g., alkali sulfate), but also reaction products (e.g., alkali hydroxides) formed from other reactions with the combustion gas constituents, as well as dissociation products such as alkali oxide and atomic alkali. The complex gas phase composition for a single-component condensate can, of course, be calculated by using local thermochemical

Table 2. K_2SO_4 Decomposition

Species i	ΔG^0 1,200 K	ΔG^0 1,300 K	ΔG^0 1,460 K
$K_2SO_{4(l)}$	−216.892	−203.516	−182.369
$K_{(g)}$	0	0	0
SO_2	−65.582	−63.84	−61.662
O_2	0	0	0
$\ln K = -(\Delta G^0/RT)$	−63.46	−54.07	−41.6
$p_{SO_2} \times 10^7$	0.911	9.53	214
$p_{K_2SO_4} \times 10^7$	6.793	73.9	4,690
$p^c_{K_2SO_4} \times 10^7$	7.7	73.9	4,900

Table 3. Input for CEC; T = 1,240 K, p = 1 atm

Species and Mole Fraction					
C_3H_8	O_2	N_2	Na_2SO_4	K_2SO_4	H_2O
2.47(−2)	4.67(−1)	4.95(−1)	8.5(−7)	1.7(−6)	9.83(−3)

equilibrium computer codes. However, to simplify calculations of vapor deposition and condensate evaporation rates in such environments we present an alternative methodology in which we introduce the concept of effective vapor pressure. Specifically, it is convenient to define an "equivalent" or "effective" partial pressure of each sulfate,

$$p^e_{M_2SO_4} \equiv \sum_{i=1}^{N} \frac{1}{n_i} p_i \tag{9}$$

that is,

$$p^e_{M_2SO_4} \equiv p_{M_2SO_4} + \frac{1}{2} p_M + \frac{1}{2} p_{MOH} + \cdots$$

where p_i is the vapor pressure of species i-containing alkali element and n_i is a stoichoimetric coefficient determined simply by the number of M atoms per molecule of species i. $p^e_{M_2SO_4}$ can also be regarded as twice the alkali element "solubility" in the gas mixture (Liang et al., 1986). Then we obtain an almost linear relationship between the logarithm of the effective partial vapor pressure and reciprocal temperature:

$$\log_{10} p^e_{K_2SO_4} = 6.8113 - (15{,}236.5/T)$$
$$\log_{10} p^e_{Na_2SO_4} = 6.1167 - (14{,}901.5/T)$$

where p^e_i is expressed in atm and T in Kelvins. Now it is easy to find that whereas $p^0_{K_2SO_4}/p^0_{Na_2SO_4}$ is in the range 10–30, the ratio of $p^e_{K_2SO_4}$ and $p^e_{Na_2SO_4}$ is predicted to be only about 2.6 in the temperature range of our interest; much closer to the experimental value 1.5 inferred from the analysis of our flash evaporation data.

Table 4. Equilibrium Composition of Combustion Products

Species and Mole Fraction				
CH_2O_2	CO	CO_2	H	$HNCO$
3.98(−16)	5.36(−9)	7.26(−2)	2.90(−11)	3.95(−20)
HNO	HNO_2	HNO_3	HO_2	H_2
6.7(−12)	1.54(−8)	7.34(−11)	8.44(−8)	5.17(−9)
H_2O	H_2O_2	H_2SO_4	K	KH
1.06(−1)	2.17(−9)	9.67(−12)	8.58(−11)	7.41(−18)
K_2CO_3	K_2O	KO	KOH	$K_2O_2H_2$
1.15(−12)	5.44(−20)	1.52(−11)	2.17(−6)	5.98(−12)
K_2SO_4	N	NH	NH_2	NH_3
5.48(−7)	1.36(−17)	7.64(−20)	3.97(−19)	4.21(−17)
NO	NO_2	NO_3	N_2	N_2O
2.87(−4)	4.93(−6)	1.77(−12)	4.85(−1)	1.33(−8)
N_2O_4	Na	NaH	NaO	$NaOH$
9.27(−18)	2.53(−10)	7.65(−17)	5.91(−11)	1.11(−6)
Na_2	Na_2O	$Na_2O_2H_2$	Na_2SO_4	O
8.74(−21)	4.87(−17)	7.43(−12)	2.11(−7)	3.28(−8)
OH	O_2	O_3	SO_3	SO_2
6.07(−6)	3.36(−1)	4.83(−11)	1.62(−7)	1.48(−6)

Prediction of dewpoint, condensate composition, and deposition rate

Vapor Boundary Layer Transport Theory. The transport theory we have used to analyze the present deposition and flash-evaporation experiments has its origins in the "chemically frozen" boundary layer theory discussed in detail in Rosner et al. (1979). In the present case the important assumptions are as follows:

1. Negligible phase change (mist formation) occurs within the vapor diffusion boundary layer; that is, phase change takes place only at the macroscopic vapor/condensate interface (station w). [The subject of boundary layer phase change processes, introduced previously, is beyond the scope of this paper; it is dealt with by Castillo and Rosner (1987a–c) and Liang et al., (1987).] Thus, we can symbolize the deposition process as: $M_2SO_{4g,e} \rightarrow M_2SO_{4g,w} \leftrightarrow M_2SO_{4c}$.
2. Vapor-condensate equilibrium exists at the condensate surface. Thus, the partial pressure of each salt is compatible with the thermochemical coexistence of the condensed salt solution.
3. The mass fraction of each condensible vapor is sufficiently small so that the prevailing velocity and temperature fields are not affected by the relatively small amount of vapor.
4. All thermophysical properties of the gas mixture will be considered constant and approximately equal to values for the host gas at mainstream conditions.
5. The condensible vapor behaves like an ideal gas.

In addition, here we further assume that:

6. Sulfate vapor thermophoresis (the Soret effect; Rosner, 1980) can also be neglected, compared to Fick (concentration) diffusion.
7. To take into account nonideality of the molten salt solution, the K_2SO_4/Na_2SO_4 binary mixture is regarded as a "regular" solution so that the activity coefficient of species 1 can be expressed as an exponential function of a second species mole fraction: $\gamma_1 = \exp(\beta x_2^2)$.

For the deposition of such trace binary condensible species, which convectively diffuse toward the cold wall across an undersaturated gaseous boundary layer, we therefore expect that the molar flux of the condensible material at the wall surface can be expressed

$$-\overline{J_i''} = K_{m,i}[p^e_{i,\infty} - p^e_i(T_w)a_i], \quad i = 1, 2 \tag{10}$$

where $K_{m,i}$ is a mass transfer coefficient based on the difference of partial vapor pressure; $p^e_{i,\infty}$ is the effective partial pressure of component i in the mainstream; $p^e_i(T_w)$ is the equilibrium vapor pressure of component i at temperature T_w; $a_i = \gamma_i x_i$ is the thermodynamic activity of component i in the solution; and superscript e indicates the effective vapor pressure is introduced (to include the effects of chemical reaction with the combustion products) as defined previously. An interesting implication of our introduction of effective vapor pressure is that the present results become insensitive to the details of the vapor phase chemistry within the boundary layer, that is, our results are no longer dependent on the above-mentioned "chemically frozen" assumption. This is because the effective vapor pressure approach is equivalent to one based on chemical element concentrations, and since chemical elements are conserved in ordinary

chemical reactions, transport laws cast in terms of local element concentrations (irrespective of the species distribution) become insensitive to the vapor phase chemistry (Rosner, 1986; Rosner et al., 1987). This is especially true when all species that transport each element have comparable Fick (and Soret) diffusivities, as is nearly the case in these alkali sulfate salt-containing combustion product gas examples, provided mist formation does not occur (Liang et al., 1987).

Predicted Results and Comparison with Experimental Observations. As described earlier, the addition of a second alkali salt in the mainstream will significantly increase the dewpoint temperature. Based on the definition of dewpoint temperature, at which the net condensible species flux approaches zero, $-\dot{J}_i'' = 0$, we immediately have

$$p^e_{i,\infty} = p^e_i(T_{dp})x_i\gamma_i \quad (i = 1, 2)$$
$$\sum_{i=1}^{2} x_i = 1 \tag{11}$$

Solving Eqs. 11, we can find the dewpoint temperature T_{dp} as well as its corresponding condensate composition x_i for given deposition conditions.

The dewpoint temperatures calculated by CEC code-free energy minimization technique and by the simple method recommended above, as well as our experimental data, are plotted in Figure 5. Not surprisingly, because the CEC code used has the assumption of ideal solution of condensed phase, there is a systematic deviation between these results and those predicted by the model including solution nonideality. However, the average deviation between these two predictions is only about 5.5 K in the concentration ratio range, $r \equiv [Na_2SO_4/K_2SO_4]_{feed}$ from 0.1 to 1.0.

In our binary deposition experiments the concentration of K_2SO_4 in the feed is constant. When the molarity of potassium sulfate in the nebulizer aqueous solution is 0.0125 M, its effective partial vapor pressure in the combustion gases corresponds to about 1.7×10^{-6} atm. Considering steady state deposition at constant $p_{i,\infty}$, the molar flux ratio must satisfy the condition:

$$\frac{-\dot{J}_1''}{-\dot{J}_2''} = \frac{x_1}{x_2} \tag{12}$$

For a binary solution,

$$x_1 + x_2 = 1 \tag{13}$$

so

$$\frac{-\dot{J}_1''}{-\dot{J}_2''} = \frac{1 - x_2}{x_2} \tag{14}$$

Here,

$$-\dot{J}_i'' = K_{m,i}[p^e_{i,\infty} - p^e_i a_i]$$
$$= K_{m,i}[p^e_{i,\infty} - p^e_i\gamma_i x_i]$$
$$= K_{m,i}[p^e_{i,\infty} - p^e_i x_i \exp(\beta x_j^2)]$$

Substituting this equation into Eq. 14 and assuming $K_{m,i} \sim D_i^{2/3}$, we obtain

$$\frac{1 - x_2}{x_2} = \left(\frac{D_1}{D_2}\right)^{2/3} \cdot \frac{p^e_{1,\infty} - p^e_1(1 - x_2)\exp(\beta x_2^2)}{p^e_{2,\infty} - p^e_2 x_2 \exp(\beta(1 - x_2)^2)} \tag{15}$$

[We estimate D_1/D_2 by assuming that this ratio is close to the diffusivity ratio of the corresponding salt hydroxides in air, which is about 0.8; the $\frac{2}{3}$ power law is known to be exact when $\sqrt{Re} \gg 1$ and $Sc \geq 0(1)$ (for laminar boundary layer flow).]

In what follows it will be convenient to introduce the mainstream salt ratio r, satisfying:

$$r \equiv \frac{p^e_{2,\infty}}{p^e_{1,\infty}} \tag{16}$$

Equation 15 describes the relationship between condensate composition x_2 and deposition conditions $p_{1,\infty}$, r, and T, and it is valid until the target temperature reaches the dewpoint.

Numerically solving the nonlinear equation

$$\frac{1 - x_2}{x_2} = \left(\frac{D_1}{D_2}\right)^{2/3} \frac{p^e_{1,\infty} - p^e_1(1 - x_2)\exp(\beta x_2^2)}{rp^e_{1,\infty} - p^e_2 x_2 \exp[\beta(1 - x_2)^2]} \tag{17}$$

we estimated the mole fraction of sodium sulfate, x_2, in the binary salt solution formed at the cold target for each temperature $T_w < T_{dp}$. [As the target temperature T_w approaches the dewpoint T_{dp}, the flux ratio of these two species becomes indeterminate (zero divided by zero). Since the function $-\dot{J}_i''$ are continuous and differentiable in the domain near T_{dp} and $d\dot{J}_i''/dT \neq 0|_{T=T_{dp}}$, then, L'Hospital's role can be applied to estimate the corresponding condensate composition at the dewpoint temperature, which is identical with the results obtained from Eqs. 11.] Figures 7a and 7b show the variation of sodium sulfate mole fraction with increasing salt concentration ratio (sodium sulfate and potassium sulfate in the feed) at T_w = 1,147 and 1,173 K, respectively, where the solid lines take account of solution nonideality and the dashed lines treat the solution as ideal.

It is interesting to use our experimental data to examine the success of the K_2SO_4 deposition rate relation

$$-\dot{J}_1'' = K_{m,1}[p^e_{1,\infty} - p^e_1 x_1 \exp(\beta x_2^2)] \tag{18}$$

It is expected that solution nonideality would noticeably influence deposition rate predictions, especially when the deposition temperature is near the dewpoint. [For instance, when the mole fraction of Na_2SO_4 is 0.8, the activity coefficient of potassium sulfate in the binary solution is $\gamma_1 = \exp(\beta x_2^2) = 0.68$.]

The mass transfer coefficient $K_{m,1}$ is difficult to predict at the prevailing gas flow Reynolds number, however, we expect that it will be insensitive to T_w/T_∞ and changes in seed level. Therefore, we proceed by selecting an experimentally measured data point as a match point and then use the theory to predict potassium sulfate deposition rate trends. The results, and our experimental measurements, are shown in Figure 3. The dotted lines display corresponding results obtained using the ideal solution model. Except for some systematic deviations at the lowest target temperature shown, Eq. 18 is seen to describe our deposition rate trends rather well.

Conclusions

Our experimental studies of K_2SO_4/Na_2SO_4 binary salt vapor deposition processes demonstrate that the flash-evaporation technique developed and exploited in this laboratory is a simple yet rather powerful experimental method to study high-temperature multicomponent deposition/evaporation processes. It is

low-cost, rather accurate, and rapid, and it provides the opportunity to investigate several species at the same time without mutual optical interference. As implemented here, the method has not only provided dewpoints, condensate compositions, and chemical vapor deposition rates, but also insight into the vapor phase chemistry (alkali hydroxide formation), and the chemical thermodynamics of such condensate solutions.

We have provided experimental evidence that the deposition and vaporization processes of alkali sulfates at high temperatures are not simply physical phase change processes, but are strongly influenced by chemical reactions, especially in combustion gas mixtures containing H_2O, O_2, ... In other words, one must consider these processes to be chemical vapor deposition (CVD) and chemical evaporation processes. Combustion conditions (such as fuel/air ratio) will therefore influence the deposition behavior of such inorganic compounds in a combustor. For the K_2SO_4/Na_2SO_4 binary system the following chemical reactions play an important role in the deposition/evaporation processes:

$$M_2SO_{4(c)} = 2M_{(g)} + SO_{2(g)} + O_{2(g)}$$
$$M_2SO_{4(c)} + H_2O_{(g)} = 2MOH_{(g)} + SO_{2(g)} + \tfrac{1}{2}O_{2(g)}$$
$$M_2SO_{4(g)} + CO_{2(g)} = M_2CO_{3(g)} + SO_{2(g)} + \tfrac{1}{2}O_{2(g)}$$

along with the physical vaporization equilibrium:

$$M_2SO_{4(c)} = M_2SO_{4(g)}$$

where M = Na or K. To simplify engineering computations of multisalt deposition and evaporation rates and to make the results insensitive to the details of the homogeneous chemical kinetics, we suggest the use of an effective vapor pressure to allow for such chemical reactions, that is,

$$p^e_{M_2SO_4} \equiv \sum_{i=1}^{n} \frac{1}{n_i} p_i = p_{M_2SO_4} + \frac{1}{2} p_M + \frac{1}{2} p_{MOH} + \cdots$$

In the present cases the effective partial pressure is simply twice the total alkali element pressure (solubility) in the prevailing gas mixture. Thus, based on our flash curve analysis we estimate that the relative volatility of K_2SO_4/Na_2SO_4 is only about 1.5, Figure 10, close to $p^e_{K_2SO_4}/p^e_{Na_2SO_4}$ defined above, whereas without taking account the chemical reactions involved, the $p^0_{K_2SO_4}/p^0_{Na_2SO_4}$ ratio in this temperature range is as high as 10–30. This simple method can be extended to other thermochemical systems, thereby minimizing the need to make repetitive use of codes to compute multicomponent chemical equilibria, provided "intersalt" compounds (e.g., $M_1M_2SO_4$) are unimportant (Liang et al., 1986).

Experimental observations presented in this paper are quantitatively consistent with the deposition rate trends predicted by a simple mist-free boundary layer mass transfer theory, according to which differences in effective vapor pressure comprise the approximate driving force for mass transfer; that is, for the primary salt 1: $-\dot{J}''_1 \cong K_{m,1}[p^e_{1,\infty} - a_1 p^e_1(T_w)]$. However, when experimental conditions are changed enough (say, by lowering the deposition target temperature and/or increasing the additive/primary ratio), the mist-free boundary layer assumption eventually breaks down. In such cases the simple boundary layer transport theory used here must be modified to include the formation/transport of a condensate "mist," as reported in our further publications (Liang et al., 1987; Castillo and Rosner, 1987c). In any case, our flash evaporation experiments suggest that binary alkali sulfate salt solutions can be conveniently described using "regular" nonideal solution theory. For a binary mixture of K_2SO_4 and Na_2SO_4, the activity coefficient of the two components can therefore be written:

$$\gamma_1 = \exp(\beta x_2^2)$$
$$\gamma_2 = \exp(\beta x_1^2)$$

where our flash-evaporation experiment composition 'trajectories' suggest an interaction parameter β near -0.6, not far from that determined from previous independent thermochemical measurements. Even though it is well known that the thermochemical properties of potassium are rather similar to those of sodium, this modest level of nonideality should still be taken into account, since it causes systematic deviations in predicting dewpoints, deposition rates, and deposit compositions. In the present case we find that the average dewpoint temperature deviation due to nonideality is about 5.5 K for feed concentration ratios $[Na_2SO_4/K_2SO_4]$ between 0.1 and 1.0.

In conclusion we should remark that the conditions of our multicomponent flash-evaporation experiments are deliberately much simpler than those encountered in combustion turbines, power stations, and many other CVD systems of current technological interest. Yet, the techniques developed and outlined here have been shown to be capable of providing experimental data useful to systematically test important facets of a theoretical approach that can be adapted economically to more extreme conditions. This same strategy underlies our current laboratory and theoretical studies of the interactions between particle deposition (Rosner and Kim, 1984) and vapor deposition in high-temperature flow systems (Rosner and Liang, 1986; Castillo and Rosner, 1987c; Rosner, 1987).

Acknowledgment

We have benefited from useful discussions and/or correspondence with R. Atkins, B. Halpern, D. Frey, J. Castillo, R. Nagarajan, F. J. Kohl, and C. A. Stearns. R. Roy assisted with the flash curve analysis. This research, which also provided the basis for Paper 62c at the 1986 AIChE Annual Meeting (11/5/86, Miami Beach, FL), was supported at Yale by NASA (Lewis Lab) and Department of Energy (METC) under Grant Nos. NAG 3-590 and DE AC21-85MC22075, respectively.

Notation

A_i = integration area of flash curve for species i
a_i = thermodynamic activity of species i in alkali sulfate solution
D_i = Fick diffusion coefficient of species i in prevailing combustion gas mixture
f_i = function, Eq. 2
ΔH^{mix} = molar heat of mixing for alkali sulfate solution
I_i = atomic emission intensity for species i
J''_i = molar flux of vapor species i from/to condensate layer
K = reaction equilibrium constant
$K_{m,i}$ = mass transfer coefficient, based on difference of species i partial pressure across boundary layer
p = total pressure in system
p_i = partial pressure of species i
p^0_i = equilibrium partial pressure of undissociated species i
p^e_i = effective vapor pressure, Eq. 9
R = universal gas constant
R_i = function, Eq. 8
r = mainstream salt ratio

S = dimensionless sensitivity coefficient
Sc_i = Schmidt number, ν/D_i
T = temperature, K
t = time
x_i = mole fraction of species i in condensate solution

Greek letters

α = relative volatility of the two salts
β = interaction parameter defined in regular solution theory
γ_i = activity coefficient

Subscripts

dp = dewpoint
i = salt or alkali species
w = at the wall (vapor/condensate interface)
∞ = in the mainstream

Literature Cited

Blander, M., *Molten Salt Chemistry,* Interscience, New York (1964).

Castillo, J. L., and D. E. Rosner, "Theory of Surface Deposition from a Unary Dilute Vapor-Containing Stream Allowing for Condensation within the Laminar Boundary Layer," *Chem. Eng. Sci.,* (1987a).

———, "Theory of Surface Deposition from Particle-Laden, Dilute, Saturated Vapor-Containing Streams Allowing for Particle Thermophoresis and Vapor Scavenging within the Boundary Layer," *Chem. Eng. Sci.,* (1987b).

———, "Nonequilibrium Theory of Surface Deposition from Particle-Laden, Dilute Condensible Vapor-Containing Streams, Allowing for Particle Thermophoresis and Vapor Scavenging within the Laminar Boundary Layer," *Int. J. Multiphase Flow,* (1987c).

———, "Theory of Surface Deposition from a Binary Dilute Vapor-Containing Stream, Allowing for Equilibrium Condensation within the Laminar Boundary Layer," *Int. J. Multiphase Flow,* (1987).

Cubicciotti, D., and F. J. Keneshea, "Thermodynamics of Vaporization of Sodium Sulfate," *High Temp. Sci.,* **4,** 32 (1972).

Cutler, A. J. B., "Molten Sulfates," *Molten Salt Techniques,* Plenum, New York, 111 (1983).

Fryxell, R. E., C. A. Trythall, and R. J. Perkins, "Vapor Pressure of Liquid Sodium Sulfate from 954 to 1204°C," *Corrosion,* NACE, 423 (1973).

Gordon, S., and B. J. McBride, "Computer Program for Calculation of Complex Chemical Equilibrium Compositions, Rocket Performance, Incident and Reflected Shocks, and Chapman-Jouguet Detonations," Tech. Rept. NASA SP-273, NASA Lewis Research Center (1976).

Gorokhov, L. N., "Annual Report, Institute for High Temperatures," USSR Acad. Sci. (1975).

Hastie, J. W., *High Temperature Vapors,* Academic Press, New York (1975).

———, "Alkali Vapor Transport in Coal Conversion and Combustion Systems," Tech. Rept. 81-2279, U.S. Dept. Commerce–Nat. Bur. Standards (1981).

Janz, G. J., C. B. Allen, N. P. Bansal, R. M. Murphy, and R. P. T. Tomkins, "Physical Properties Data Compilations Relevant to Energy Storage," Tech. Rept. NSRDS-NBS 61, Pt. 2, U.S. Dept. Commerce–Nat. Bur. Standards (1979).

Kohl, F. J., G. J. Santoro, C. A. Stearns, G. C. Fryburg, and D. E. Rosner, "Theoretical and Experimental Studies of the Deposition of Na_2SO_4 from Seeded Combustion Gases," *J. Electrochem. Soc.,* **126,** 1054 (1979).

Lau, K. H., D. Cubicciotti, and D. L. Hildebrand, "Effusion Studies of the Vaporization/Decomposition of Potassium Sulfate," *J. Electrochem. Soc.: Solid-state Sci. Technol.,* **126,** 490 (1979).

Liang, B. "Experimental Studies of Multicomponent Salt Vapor Deposition Rate Processes Using a Flash-Evaporation Technique," Ph.D. Diss., Dept. Chem. Eng., Yale Univ. (1987).

Liang, B., R. Roy, and D. E. Rosner, "Simplification of Multisalt Dewpoint Predictions Allowing for Salt-Combustion Product Chemical Reactions and Solution Nonideality," *J. Electrochem. Soc.,* submitted (1986).

Liang, B., A. Gomez, J. L. Castillo, and D. E. Rosner, "Experimental Studies of Nucleation Phenomena within Thermal Boundary Layers—Influence on Chemical Vapor Deposition Rate Processes, *AIChE J.,* submitted (1987).

Lumsden, J., *Thermodynamics of Molten Salt Mixtures,* Academic Press, London (1966).

Ostvold, T., and O. J. Kleppa, "Enthalpies of Mixing in Binary Liquid Alkali Sulfate Mixture," *Acta Chem. Scand.,* **25,** 919 (1971).

Powell, C. F., J. H. Oxley, and M. B. Blocher, Jr., *Vapor Deposition,* Wiley, New York (1966).

Robinson, McD., C. H. J. van den Brekel, G. W. Cullen, J. M. Blocher, Jr., and P. Rai-Choudhury, *9th Int. Conf. Chem. Vapor Deposition, 1984 Symp.,* Electrochem. Soc., Pennington, NJ, (1985).

Rosner, D. E., "Thermal (Soret) Diffusion Effects on Interfacial Mass Transport Rates," *Physico-Chemical Hydrodynamics* (Pergamon), **1,** 159 (1980).

———, *Transport Processes in Chemically Reacting Flow Systems,* Butterworths, New York, (1986).

———, "Experimental and Theoretical Studies of the Deposition of Inorganic Compounds from Combustion Gases," submitted (1987).

Rosner, D. E., and S. S. Kim, "Optical Experiments on Thermophoretically Augmented Submicron Particle Deposition from "Dusty" High-Temperature Gas Flows," *Chem. Eng. J.,* **29,** 147 (1984).

Rosner, D. E., and B. Liang, "Laboratory Studies of the Deposition of Alkali Sulfate Vapors from Combustion Gases Using a Flash-Evaporation Technique," *Chem. Eng. Commun.,* **42,** 171 (1986).

Rosner, D. E., and R. Nagarajan, "Transport-Induced Shifts in Condensate Dewpoint and Composition in High-Temperature Multicomponent Systems with Chemical Reaction," *Chem. Eng. Sci.,* **40,** 177 (1985).

Rosner, D. E., B. K. Chen, G. C. Fryburg, and F. J. Kohl, "Chemically Frozen Multicomponent Boundary Layer Theory of Salt and/or Ash Deposition Rates from Combustion Gases," *Comb. Sci. Technol.,* **20,** 87 (1979).

Rosner, D. E., R. Nagarajan, M. Kori, and S. A. Gokoglu, "Maximum Effect of Vapor Phase Chemical Reactions on CVD Rates and Deposition Onset Conditions in the Absence of Interfacial Chemical Kinetic Barriers," *10th Int. Conf. Chem. Vapor Deposition,* Abstract No. 1030, b1 (Oct., 1987).

Seshadri, K., and D. E. Rosner, "Optical Methods and Results of Dewpoint and Deposition Rate Measurements in Salt/Ash-Containing Combustion Gases—$B_2O_3(l)$ Deposition Rates by Interference Methods and Comparison with Theory, *AIChE J.,* **30**(2), 187 (1984).

Stearns, C. A., Kohl, F. J., and D. E. Rosner, "Combustion System Processes Leading to Corrosion Deposits," *High Temperature Corrosion,* Nat. Ass. Corrosion Eng., 441 (1983).

Stevens, C. G., and D. Tidy, "Mechanisms of Deposition of Sodium, Vanadium and Magnesium under Gas Turbine Conditions," *J. Inst. Energy,* **56,** 12 (1983).

Turkdogan, E. T., *Physical Chemistry of High Temperature Technology,* Academic Press, New York (1980).

Manuscript received Aug. 5, 1986, and revision received July 13, 1987.